

Automatic Planning Algorithms for 300 GHz Wireless Backhaul Links

Bo Kum JUNG^{†a)} and Thomas KÜRNER^{†b)}, *Nonmembers*

SUMMARY With the increasing densification of 5G and future 6G networks high-capacity backhaul links to connect the numerous base stations become an issue. Since not all base stations can be connected via fibre links for either technical or economic reasons wireless connections at 300 GHz, which may provide data rates comparable to fibre links, are an alternative. This paper deals with the planning of 300 GHz backhaul links and describes two novel automatic planning approaches for backhaul links arranged in ring and star topology. The two planning approaches are applied to various scenarios and the corresponding planning results are evaluated by comparing signal to interference plus noise ratio under various simulation conditions including weather impacts showing the feasibility of wireless backhaul links.

key words: backhaul network, backbone network, 300 GHz wireless backhaul links, THz links, backhauling topology

1. Introduction

With the evolution of wireless communication towards the 5th (5G) and future 6th (6G) generation, the pattern of data usage is transforming into high data traffic consuming services, such as video streaming, augmented or virtual reality applications, for example. In [1], 5G use cases are introduced including high speed mobile access over 50 Mbps everywhere, massive internet of things, extreme real time communications and ultra reliable communications. The total amount of global mobile data traffic including fixed wireless access service is expected to exceed even 300 Exabyte per month by 2026, which is about five times increased value compared with the total global traffic per month at the end of 2020 based on [2]. To ensure the full support of this unprecedented high data rate at the wireless access level, several categories of key elements are introduced in [3] enabling the required system's capacity increase. One of those key elements is ultra cell densification.

The large number of those ultra-dense cells require a connection to the core network via ultra-high data rate backhaul links. Since not all base stations can be connected via fibre links for either technical or economic reasons, wireless connections at 300 GHz, which may provide data rates comparable to fibre links, are an alternative.

Many of researches [4]–[8] present the planning meth-

ods of a hybrid mobile network coexisting both fibre and wireless backhaul links. The operation of those algorithms is however limited by either at micro- or at mm-Wave frequency bands. Thus, those algorithms neither consider nor address the distinctive properties of the wave propagation at sub-mm frequencies. Even though [9] presents an automatic planning wireless backhaul network operating at 300 GHz, the proposed algorithm plans wireless backhaul networks progressively by arbitrarily searching the next positions of base stations. It cannot plan the stationary network where the positions of base stations are already assigned for future installations. Apart from that, the scales of all those works are limited by rather small scenarios considering only limited numbers of base stations.

This paper provides an analysis and comparison of the two automatic planning algorithms for 300 GHz wireless backhaul links described in [10] and [11] using five different scenarios covering from a low densification scenario to an ultra-high densification scenario [12].

The remaining part of the paper is structured as follows: In Sect. 2, the two automatic planning algorithms will be introduced. The subsequent Sect. 3 describes the five network deployment scenarios used in this analysis. Section 4 contains the results of the automatic planning as well as system-level simulation results with respect to the signal to interference noise ratio (SINR) taking into account various weather conditions and system bandwidths. In Sect. 5, a brief conclusion is given.

2. Automatic Planning Algorithm

In this section, two novel approaches, with which wireless backhaul links of the given cellular network can be automatically arranged, are presented based on two different topologies: Star topology and Ring topology. Both algorithms are developed for the automatic planning of wireless backhaul network by taking into account the properties of wave propagation at THz frequencies regardless of the network size and the cell deployment. Its features are distinguishable with any other network planning tools that have been introduced previously. The goal of the algorithms is to reduce the total number of fibre backhaul links by identifying cell sites within the network, whose backhaul links can be substituted by 300 GHz wireless connections. To accomplish it, both algorithms sequentially assign the anchor cell sites with fibre backhaul, which can provide the largest number of wireless links.

Manuscript received July 6, 2021.

Manuscript revised October 11, 2021.

Manuscript publicized December 3, 2021.

[†]The authors are with the Institut für Nachrichtentechnik, Technische Universität Braunschweig, Schleinitzstraße 22, 38106 Braunschweig, Germany.

a) E-mail: bokumjung@ifn.ing.tu-bs.de

b) E-mail: kuerner@ifn.ing.tu-bs.de

DOI: 10.1587/transcom.2021SI0002

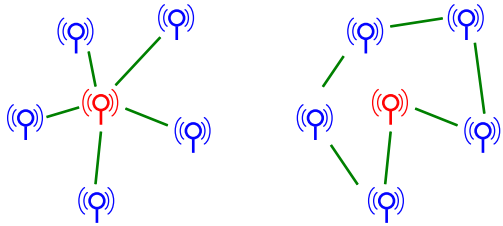


Fig. 1 Conceptual images of two backhaul networking topologies: star topology (left), ring topology (right), blue nodes are connected by wireless backhaul links to the nodes coloured in red, which are connected to a fibre backhaul link.

The conceptual images of two topologies, star and ring respectively, are visualized in Fig. 1, where the red nodes indicate anchor cell sites with fibre backhaul connection, which provides wireless backhaul links to the blue nodes.

Star topology is one of the most uncomplicated network topology to plan entire nodes. The expansion and reduction of the network's size (i.e., the total number of nodes) can be accomplished with less additional efforts since the nodes are separately connected to the central hubs. In wireless backhaul network, hubs refer to the cell sites with fibre backhaul links (anchor cell sites) and the nodes are matched to the cell sites, whose backhaul links are fed by corresponding anchor sites via one hop connection wirelessly.

Ring topology is a networking logic, whose data traffic path forms a closed circle. Each node possesses two distinctive data traffic paths to all other nodes in the ring. This property leads to the redundant paths. Thus, the backhaul network based on ring topology is more stable against a link failure due to two individual traffic paths than one based on star topology.

Planning algorithms based on both topologies share the same two input parameters: maximum link distance and a safety angle margin. The maximum link distance limits the maximum allowed path loss, so that the signal's received power can exceed the receiver sensitivity. The safety angle margin is the minimum guard angle between two adjacent THz links in order to avoid interference within a small angle within the overlap of the antenna's main lobes. Based on the position of each cell site various fundamental sets of cell sites are defined: Set A and B for star topology and set D for ring topology. Set A refers to the cell sites with already existing fibre backhaul connections (e.g., 4G cell sites) and Set B refers to newly deployed cell sites, which require a backhaul connections and Set D refers to the collection of all cell sites including cell sites with already existing fibre backhaul connections as well as no designated backhaul connections.

2.1 Automatic Algorithm for Star Topology

A simplified flow diagram of the automatic planning algorithm based on star topology is given in Fig. 2 and its decision steps are described in below and further details about automatic planning algorithm based on star topology is published in [10].

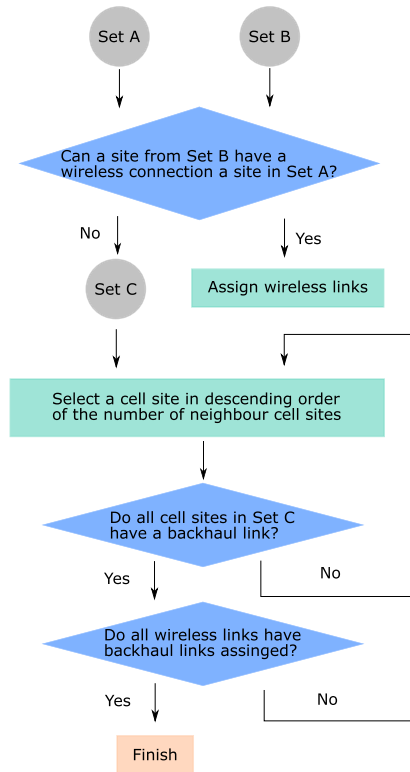


Fig. 2 Simplified decision flow diagram of the automatic planning algorithm using star topology.

1. The algorithm tries to find out possible wireless links between set A and set B taking into account safety the angle constraints, maximum link distance and availability of line-of-sight (LoS) conditions.
2. The algorithm filters cell sites from set B and create set C, which contains all cell sites, for which a wireless backhaul link to an already fibre connected cell site is not available due to the above mentioned constraints.
3. The algorithm tries to serially find anchor cell sites from set C, which surely require fibre backhaul links to provide wireless backhaul links to the other cell sites so that all cell sites in set C can be covered by either fibre or wireless backhaul links.
4. The algorithm tries to assign potential wireless links considering angle constraint and link distance.
5. If some of cell sites are not able to have potential wireless links due to angle constraint, gather those cell sites and run step 3 and step 4 iteratively until each cell site in set C can have a backhaul link.

2.2 Automatic Algorithm for Ring Topology

A simplified flow diagram of the automatic planning algorithm using ring topology is given in Fig. 3. The sequence of algorithm's decision steps is described below. Further details regarding to the algorithm can be found in [11].

1. The algorithm generates neighbourhood matrix among

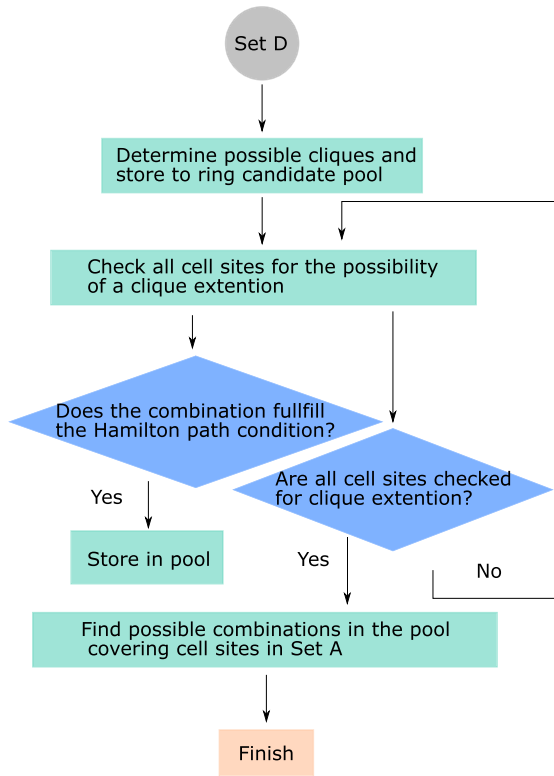


Fig. 3 Simplified decision flow diagram of the automatic planning algorithm using ring topology.

given cell sites set D considering link distance and LoS.

2. The algorithm searches for all maximum cliques using Bron-Kerbosch algorithm [13].
3. The algorithm tries to extend cliques by checking the Hamiltonian path. The clique extension is done cell site by cell site ($N_k=1, 2, \dots, k$) by gathering all cliques containing the currently checking cell site (N_i), as well as, all cliques with clique number two since a combination of such cliques with clique number two can build a closed circle. The algorithm checks all combinations of collected cliques. The combinations are stored in pool once it satisfies Hamiltonian path.
4. The algorithm tries to find possible ring candidates in the pool until all backhaul links in set D are covered.

3. Simulation Requirements

This section describes the requirements for simulations. Here, the general information about the used five scenarios are briefly described and the in-house developed simulation tool including the 300 GHz propagation model is introduced. In addition, the channel model for 300 GHz wave propagation, 3D radiation pattern, as well as the interference plus noise model will be discussed further.

3.1 Scenarios

In this paper, the two introduced automatic planning algo-

rithms are applied in five scenarios defined in [12]: Hanover, Shinjuku, Berlin-Mitte, Berlin-Kurfürstendamm and Berlin-Dahlem. Each scenario represents different small cell deployment cases with various city profiles. Each scenario contains a number of macro cell sites (MCS), which are already connected via fibre link and new deployed small cell sites (SCS), for which backhaul links have to be planned.

The Hanover scenario describes a throughput hungry area with highly deployed cell sites within relative small dimension of $1 \text{ km} \times 1 \text{ km}$ and thus it represents an ultra high deployment scenario. Totally 307 cell sites including 7 macro cell sites (MCS) and 300 small cell sites (SCS) are artificially positioned above the rooftop of buildings in this scenario.

The Shinjuku scenario covers $2.1 \text{ km} \times 2.1 \text{ km}$ area centre of Shinjuku in Tokyo and describes a typical megacity, where skyscrapers are concentrated in the middle. Within the scenario 40 MCSs are positioned above the rooftop of the buildings and 400 SCSs are located at the street level (e.g., lamp site or utility pole).

The Berlin-Mitte scenario is a throughput intensive area where business area, shopping promenade and sight-seeing attractions are sited within $2.5 \text{ km} \times 2.5 \text{ km}$ middle of Berlin area. In this area, 238 cell sites are placed including 62 MCSs and 176 SCSs. All MCS and 88 SCSs (the half of SCSs) are positioned above the rooftop of buildings while the rest of SCSs are placed at the street level.

The Berlin-Kurfürstendamm scenario is one of the typical around city areas, where business area, shopping centre and residential area are well mixed in $2.5 \text{ km} \times 2.5 \text{ km}$ area. In this scenario, 26 MCSs and 120 SCSs, entirely 146 cell sites, are arranged. Same like Berlin-Mitte scenario, 50% of SCSs are placed at the street level while MCSs and the rest of SCSs are installed above the rooftop of the buildings.

The Berlin-Dahlem scenario represents a typical residential area near city centre. Here, 274 cell sites inclusive 14 MCSs and 260 SCSs are assumed. Likewise for both other Berlin scenarios mentioned above, 50% of SCSs, exactly 130 SCSs, are positioned at the street level while the rest SCSs and MCSs are positioned above the rooftop of buildings.

3.2 Simulation Tool

To plan and evaluate the wireless backhaul networks, we used an in-house developed holistic simulation tool, known as SiMoNe (Simulator for Mobile Networks). SiMoNe is initially developed for simulating performances of realistic mobile networks [14] and functions of SiMoNe has been continuously developed and extended to the link level simulation [15]. Both link level and system level simulation are based on 3D ray optical methods considering 3D building information and 3D antenna diagrams (radiation patterns).

3.3 Propagation Channel Model

At the 300 GHz frequency range additional wave propaga-

tion have to be considered, which are not relevant at sub-6G frequency bands namely atmospheric effects. [16] suggests that at least three effects should be embodied in the propagation channel model:

- Impact of the atmospheric gases [17]
- Impact of rain [18]
- Impact of the cloud and fog [19]

In addition, the use of high gain antennas in combination with movements of the antennas due to strong wind, requires the consideration of four components [20], which are embedded in the simulator and taken into account in Eq. (1)

$$\begin{aligned} \frac{a_0}{\text{dB}} = & 20 \cdot \log_{10} \frac{d}{\text{km}} + 20 \cdot \log_{10} \frac{f}{\text{GHz}} + 92.45 \\ & + (\gamma_{at} + \gamma_r + \gamma_{cl}) \cdot \frac{d}{\text{km}} + \gamma_w. \end{aligned} \quad (1)$$

where γ_{at} refers to the impact of the atmospheric gases, γ_r refers to the impact of the rain, and γ_{cl} refers to the impact of cloud and fog. Besides, the impact of wind is modelled as γ_w , which generates the degradation of the power gain by inducing the misalignment of antennas.

3.4 Radiation Pattern of Antenna

To achieve realistic simulation results, an appropriate radiation pattern of the antenna should be taken into account since no antenna except for isotropic antenna radiates electromagnetic waves with same intensity in all directions equally. Since no verified mathematical model of radiation patterns operating at 300 GHz frequencies is currently available, the mathematical models described in [21] and [22] are assumed as the baseline to design the 3D radiation pattern for 50 dBi gain antenna operating at 300 GHz.

3.5 Modelling of Interference and Noise

To assess the channel capacity's upper bounds of planned wireless backhaul links by the means of SINR, both interference and noise are considered for each link.

Interference is determined in such a way of accumulating all destructive electro magnetic waves arriving at each receivers. This can be done by determining all propagation paths existing in the given network using ray optical method (i.e., if N numbers of cell sites are given, (N-1)! numbers of cell sites pair combinations are examined to figure out the propagation paths) and predicting their powers considering the antenna's 3d radiation pattern. The equivalent antenna's gain of each propagation path is determined by the angle difference between the rays' AoA/AoD and the pointing vector of the antenna. Figure. 4 visualizes the way to determine the effective antenna gain. The effective antenna's gain can be determined by finding the corresponding value from the 3D radiation pattern considering the angle difference.

Apart from the interference, we assumed an additional thermal noise for simulations generated by electrical circuits on the devices (e.g., -77 dBm for 5 GHz bandwidth

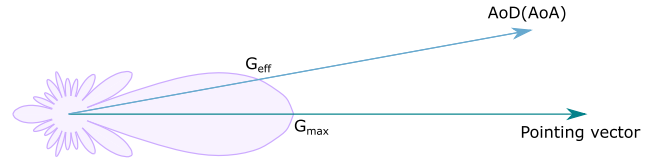


Fig. 4 Graphical representation of the ray's effective antenna gain.

Table 1 Configuration parameters for automatic planning algorithms.

	Antenna height	Safety angle margin	Link distance	Hops
Star	1 m	4 degree	300 m	n/a
Ring				6

and -67 dBm for 50 GHz bandwidth).

4. Simulation Results

4.1 Network Planning Results

We conducted the wireless backhaul planning using both provided algorithms in the five target scenarios introduced in Sect. 3.1. The configuration parameters assumed for the planning are given in Table 1.

For the planning of ring topologies an additional parameter is applied namely the number of hops. This refers to the maximum allowed number of nodes, which build a closed circular traffic path.

The corresponding planning results of wireless backhaul networks according to scenarios and topologies are visualized in Fig. 5 and Fig. 6. In each figure, the anchor cell sites (i.e., cell sites with fibre backhaul links) are represented as red dots. The cell sites, whose backhaul links connected via wireless, are represented as blue dots. The wireless links are visualized as green lines. Please note that the anchor cell sites of ring candidates are not indicated in Fig. 5 and Fig. 6 since any cell site in the ring candidates can flexibly serve the roll of the anchor cell site to provide wireless backhaul links due to closed circular traffic path.

In the Hanover scenario, 77% of cell sites can substitute their backhaul links via fibre to wireless using star topology, while 52% of cell sites can be possibly fed via wireless backhaul links using ring topology. Shinjuku scenario showed almost comparable results with Hanover scenario. 78% of cell sites can substitute their backhaul links via fibre to wireless using star topology, while 50% of cell sites can profit wireless backhaul links using ring topology. In Berlin-Mitte scenario, 59% of cell sites can utilize wireless backhaul links using star topology, while 28% of cell sites can utilize using ring topology. Berlin-Kurfürstendamm scenario showed the inferior results with respect to the algorithm's efficiency. 36% of cell sites can substitute their backhaul links via fibre to wireless using star topology, while only 15% of cell sites are available to feed wireless backhaul links using ring topology. In Berlin-Dahlem scenario, 52% of cell sites are adequate to substitute their backhaul links via fibre to wireless using star topology, while 25% of cell sites are feasible to apply wireless back-

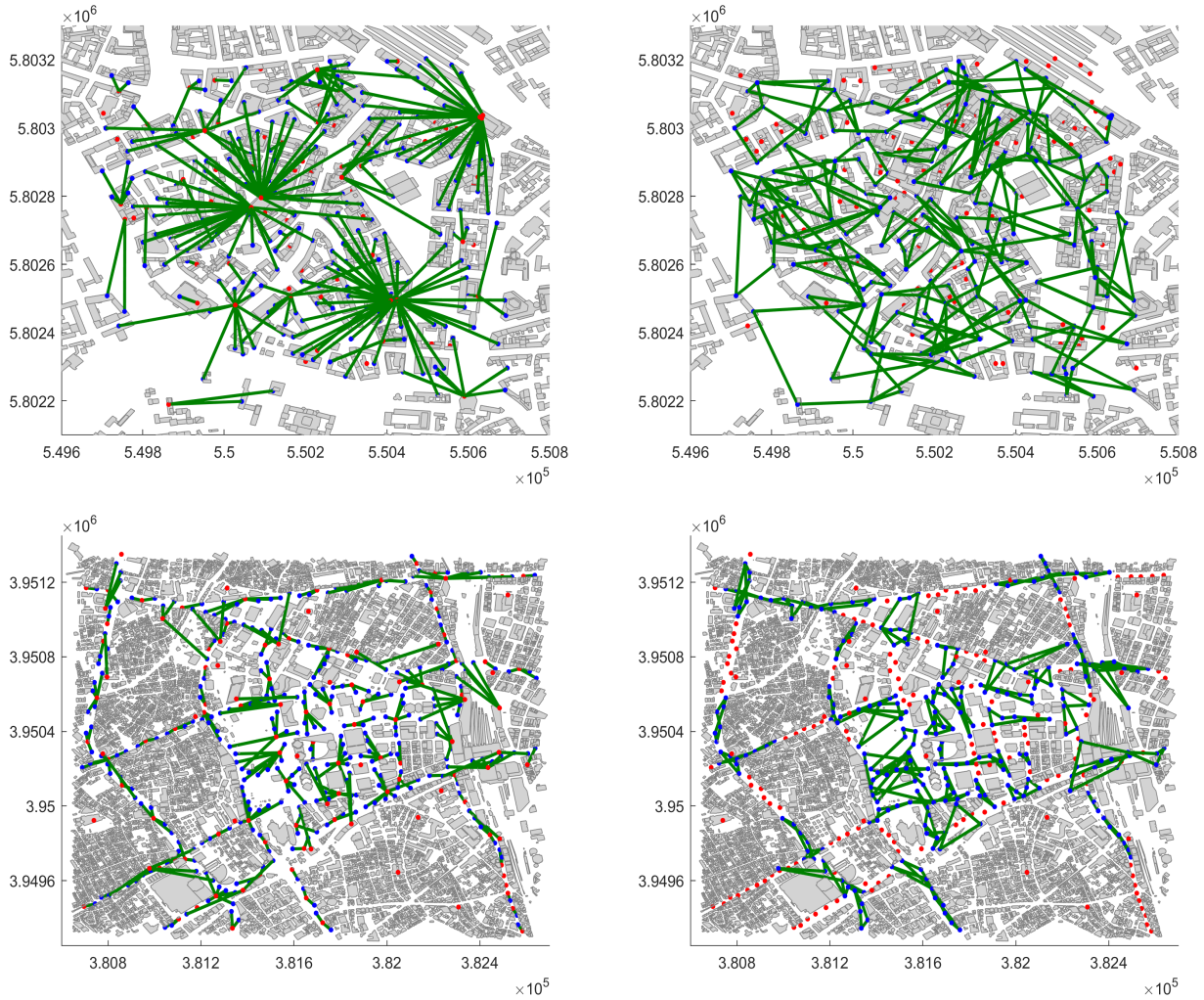


Fig. 5 Planning results of wireless backhaul network: star topology in Hanover area (left upper), ring topology in Hanover area (right upper), star topology in Shinjuku area (left under), ring topology in Shinjuku area (right under).

haul links using ring topology.

In every scenario the star topology showed better performance in terms of substituting fibre backhaul links when compared to the solutions in ring topology. The percentage of wireless backhaul possible cell sites using star topology spans between 36%–78%. The percentage using ring topology varies from 15% in worst case to 52%. More networking results considering various configuration parameters for each scenario are provided in [23].

One thing to note is the network planning result in Hanover area visualized in Fig. 5 (left upper). Here, most of wireless links are concentrated to several anchor cell sites. This is because that the optimization factor for simulations was set as reducing the number of required fibre backhaul links. The algorithm thus decided to select those anchor sites to connect possibly many wireless backhaul links for reducing the number of fibre backhaul links since they can provide the greatest number of wireless backhaul links to other cell sites due to comparably high antenna positions. However, it implies that the total numbers of wireless links

at each anchor site become more important due to the infrastructural capacity of anchor cell sites to support the onward transmission of highly aggregated data. Thus, if necessary, the number of wireless links at each anchor cell sites should be limited to secure the data transmission’s capacity.

The different performances of wireless backhaul planning resulted above are fundamentally depending on the cell sites deployment and the configuration parameters since the possibility of wireless backhaul links is decided considering the LoS condition, the maximum allowed link distance and the safety angle conflict. This means that the potential of planning performances increase as the cell sites deployment approaches the ideal state (i.e., high cell deployment and all cell sites show LoS conditions) and as the input configurations are less strictly regulated (i.e., ∞ link distance and zero safety angle margin). Therefore, Berlin-Kurfürstendamm scenario showed the worst performance since the density of cell sites is low and they are geographically isolated due to buildings. In contrast, the Hanover scenario and Shinjuku scenario showed the best performance due to the high den-

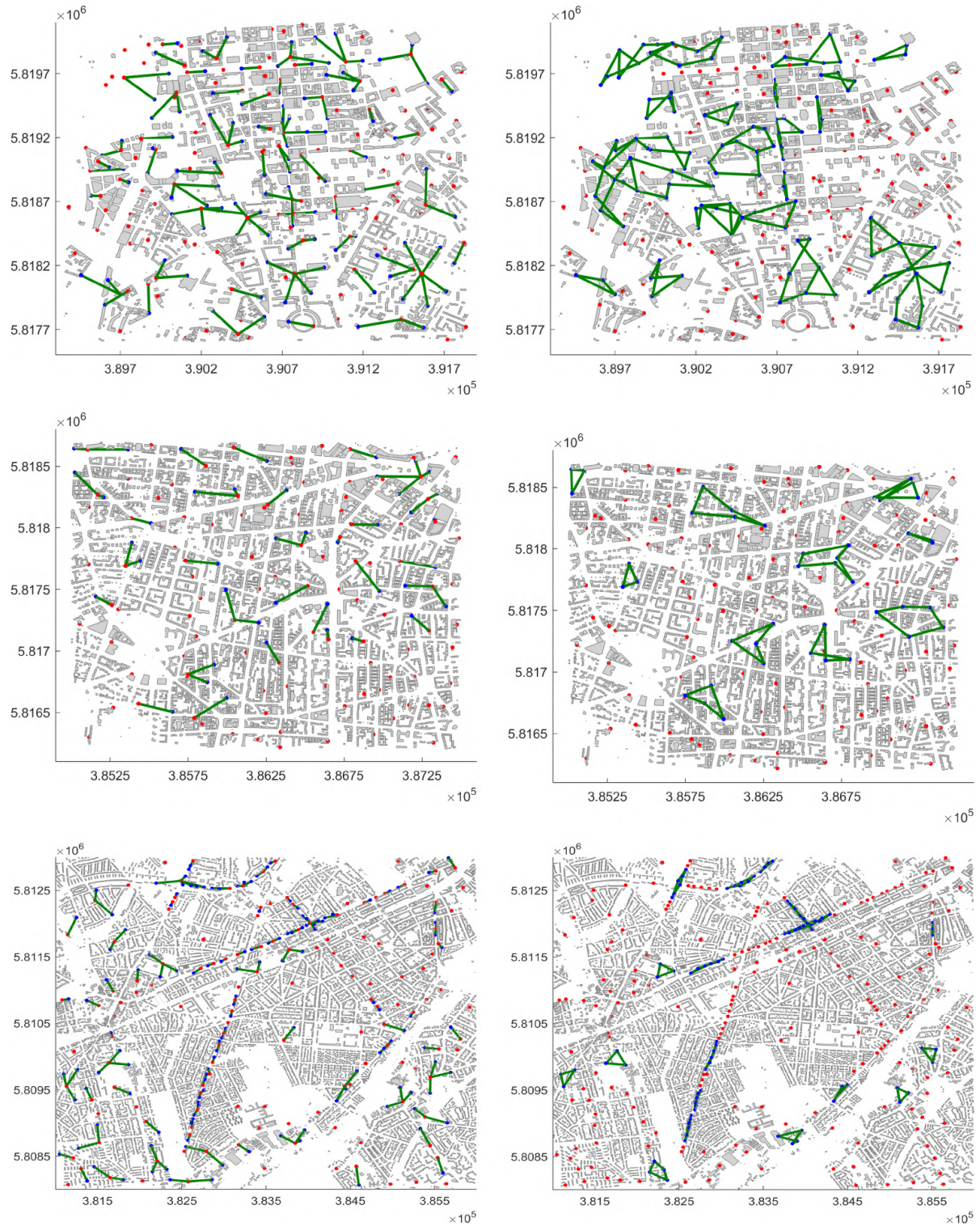


Fig. 6 Planning results of wireless backhaul network: star topology in Berlin-Mitte area (left upper), ring topology in Berlin-Mitte area (right upper), star topology in Berlin-Kurfürstendamm area (left middle), ring topology in Berlin-Kurfürstendamm area (right middle), star topology in Berlin-Dahlem area (left under), ring topology in Berlin-Dahlem area (right under).

Table 2 Hardware parameters used for system level simulations.

Parameter	Value
RF centre frequency	300 GHz
Transmission power	0 dBm
Tx antenna gain	50 dBi
Rx antenna gain	50 dBi

Table 3 Probability of THz links exceeding 22 dB to apply the highest modulation and coding scheme.

	Clear weather	Extreme weather	Extreme weather
	5 GHz bandwidth	5 GHz bandwidth	50 GHz bandwidth
	Star / Ring	Star / Ring	Star / Ring
H [†]	94% / 99.8%	94% / 99.8%	93.1% / 99.8%
S ^{††}	91.3% / 97%	91.3% / 97%	91.3% / 97%
BM ^{†††}	95.3% / 98.5%	95.3% / 98.5%	95.3% / 98.5%
BK ^{††††}	100% / 100%	100% / 100%	100% / 100%
BD ^{†††††}	90% / 94.5%	90% / 94.5%	90% / 94.5%

[†]Hanover scenario
^{††}Shinjuku scenario
^{†††}Berlin-Mitte scenario
^{††††}Berlin-Kurfürstendamm scenario
^{†††††}Berlin-Dahlem scenario

sity of cell sites and the lower rate of blocking LoS by the obstacles.

4.2 System Level Simulation Results

To investigate the quality of wireless backhaul links, we conducted system level simulations using the automatically planned backhaul networks visualized in Sect. 4.1. For that, two types of weather conditions (clear and extreme) are assumed. The clear weather refers to the clear weather neither rain nor wind. The corresponding weather parameters are set as 1013.25 hPa air pressure, 17° temperature and 7.5 g/m³. The extreme weather indicates a rainy and windy condition. The weather parameters for the extreme weather condition are formed by adding the rain segment and the wind segment based on the clear weather condition. They are artificially set as 1013.25 hPa air pressure, 17° temperature, 7.5 g/m³, 50 mm/h rain rate (heavy rain) and wind speed of 20 m/s (fresh gale) from North.

For the simulations, the hardware parameters given in Table 2 are assumed. As a results of simulations, received powers of propagation paths at each antennas are predicted using the propagation model described in Sect. 3.3.

The corresponding SINR probabilities in various scenarios are given in Figs. 7–11. In each figure, six probability curves are visualized depending on weather conditions, topologies and the bandwidth size. The standard demand of SINR value is additionally visualized as a dotted line, which corresponds to 22 dB and is the required value to apply the highest modulation and coding scheme (64 QAM 14/15 FEC) defined in [24].

In Table 3, the percentages are given how many THz links can exceed the SINR (22 dB) enabling the highest modulation and coding scheme (64 QAM 14/15 FEC) defined in [24].

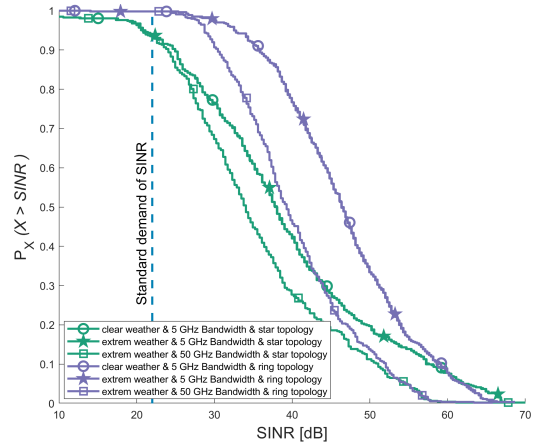


Fig. 7 SINR comparison of both planning algorithm using various weather condition in Hanover.

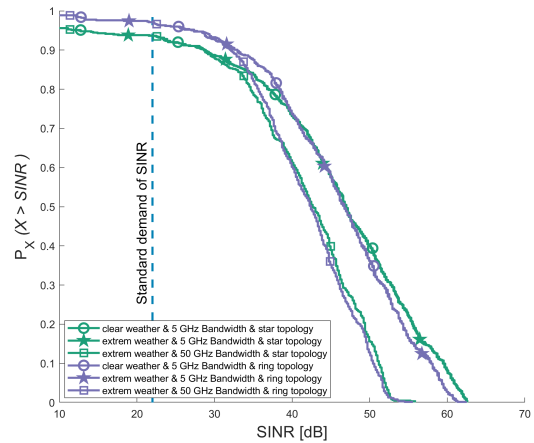


Fig. 8 SINR comparison of both planning algorithm using various weather condition in Shinjuku.

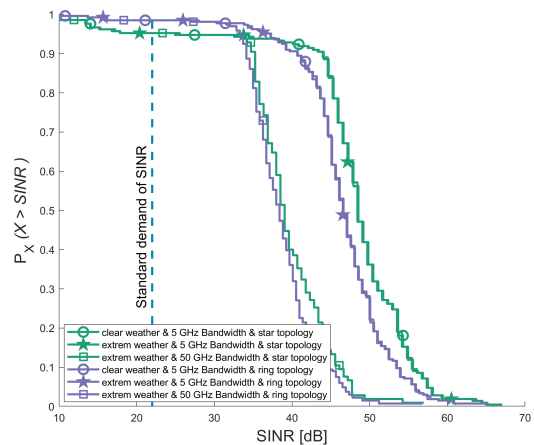


Fig. 9 SINR comparison of both planning algorithm using various weather condition in Berlin-Mitte.

The results of all five scenario showed that most of the planned wireless backhaul links are feasible to apply the highest modulation and coding scheme defined in [24].

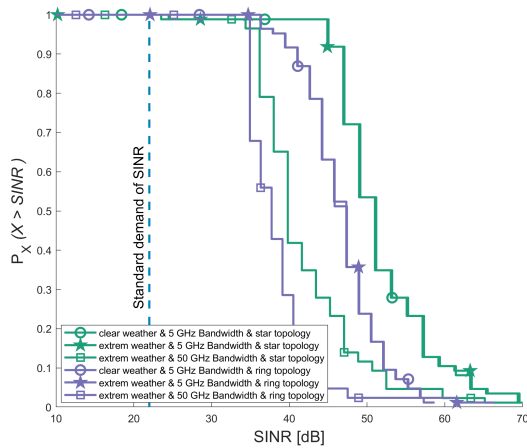


Fig. 10 SINR comparison of both planning algorithm using various weather condition in Berlin-Kurfürstendamm.

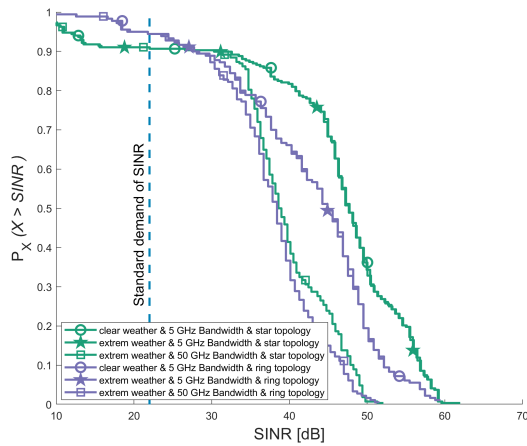


Fig. 11 SINR comparison of both planning algorithm using various weather condition in Berlin-Dahlem.

Only some of wireless links do not exceed the required value of 22 dB, which require the use of a more robust modulation and coding scheme yielding a lower data rate.

One noticeable thing in Figs. 7–11 is that no dominant impact of the weather condition using same bandwidth is observable. This is because interfere signals are the dominant part using 5 GHz bandwidth regardless of weather condition due to the short link distance. This means, both the signal and interference become simultaneously bad as the weather goes bad but both values still overwhelm the thermal noise. However, in case of 50 GHz bandwidth, the thermal noise increases 10 dB compared with using 5 GHz bandwidth. Thus, it becomes partially the dominant interferer especially for the links with high SINR since impact of weather conditions expands proportional to the distance. Therefore, the SINR curves fall more drastically at a certain point not completely shifted to the left as the bandwidth grows.

In general, using ring topology showed better SINR probability than using star topology. This is due to the number of total wireless links, as well as the number of wireless

links per nodes. More wireless backhaul links are planned using star topology than ring topology in every scenario. This leads to a higher probability of unwanted interference level, even though it is regulated at the planning step. In addition, the anchor cell sites in star topology tend to provide a large number of wireless backhaul links. This means the wireless links are rather concentrated on the certain cell site using star topology, while the links are more equally distributed to all cell sites using ring topology. This results in a potentially high aggregated interference level and thus a lower SINR. Mostly two wireless links are existing per cell site and only some of cell sites have more than two wireless backhaul links based on ring topology.

5. Conclusion

In this paper, two novel approaches for automatic planning wireless backhaul links are presented. The corresponding simulations based on both presented algorithms are conducted using five different small cell deployment scenarios. Totally ten planning results are visualized. The system level simulations of each planning result are done considering two weather conditions (clear and extreme) and two bandwidths (5 GHz and 50 GHz) to assess the planned wireless backhaul links under diverse transmission circumstances. Using the planning algorithms, from 15% up to 78% of cell sites can substitute their fibre backhaul links with wireless alternative depending on the given scenario and topology.

Each planned backhaul network showed that weather conditions and the bandwidth influence on the SINR probability, it nonetheless does not strongly impact on the applicable modulation and coding scheme. In worst case, 10% of planned wireless links are not feasible to benefit the highest modulation and coding scheme (64 QAM and 14/15 FEC) defined in IEEE Standard 802.15.3d. This shows that wireless backhaul links operating at 300 GHz are feasible and sustainable under the given extreme weather condition even using 50 GHz bandwidth.

The simulation results showed that the performance of planning wireless backhaul network is deterministic by the scenario and the input configurations. This emphasizes the importance of the appropriate deployment of small cell sites, as well as, the proper selection of input configurations. In terms of increase planning efficiency, new small cell sites should be deployed where possibly many LoS conditions are guaranteed. At the same time, new cell sites are recommended to distribute possibly fairly while maintaining the distance in certain degree.

Further relating studies will contain the simulation results of cell coverage probability using the real hardware specifications used in the demonstrator developed in the ThoR project, and will further extend the planning algorithms to NLoS wireless backhaul links.

Acknowledgments

The work presented here, has been performed within the

Horizon 2020 ThoR project. This project has received funding from Horizon 2020, the European Union's Framework Programme for Research and Innovation, under grant agreement No. 814523. ThoR has also received funding from the National Institute of Information and Communications Technology in Japan (NICT).

References

- [1] NGMN Alliance, "5G white paper," Feb. 2015.
- [2] Ericsson, "Ericsson mobility report," June 2021.
- [3] Q.C. Li, H. Niu, A.T. Papatthanasious, and G. Wu, "5G network capacity: Key elements and technologies," *IEEE Veh. Technol. Mag.*, vol.9, no.1, pp.71–78, March 2014, doi: 10.1109/MVT.2013.2295070.
- [4] B. Marques, M. Sousa, P. Vieira, M.P. Queluz, and A. Rodrigues, "Automated joint access and backhaul planning for 5G millimeter-wave small cell networks," 2020 23rd International Symposium on Wireless Personal Multimedia Communications (WPMC), 2020, pp.1–6, doi: 10.1109/WPMC50192.2020.9309498.
- [5] A. Cai, G. Qiao, Y. Li, L. Shi, and G. Shen, "Multi-period topology planning for microwave-based wireless backhaul networks," 2014 Asia Communications and Photonics Conference (ACP), pp.1–3, 2014.
- [6] G.E. Athanasiadou, P. Fytampanis, D.A. Zarbouti, G.V. Tsoulos, P.K. Gkonis, and D.I. Kaklamani, "Radio network planning towards 5G mmWave standalone small-cell architectures," *Electronics*, vol.9, no.2, 339, 2020, doi: 10.3390/electronics9020339.
- [7] Y. Li, G. Qiao, A. Cai, L. Shi, H. Zhao, and G. Shen, "Microwave backhaul topology planning for wireless access networks," 2014 16th International Conference on Transparent Optical Networks (ICTON), pp.1–4, 2014, doi: 10.1109/ICTON.2014.6876516.
- [8] O. Grøndalen, O. Østerbø, G. Millstein, and T. Tjelta, "On planning small cell backhaul networks," 2015 European Conference on Networks and Communications (EuCNC), pp.397–402, 2015, doi: 10.1109/EuCNC.2015.7194106.
- [9] R. Okumura and A. Hirata, "Automatic planning of 300-GHz-band wireless backhaul link deployment in metropolitan area," 2020 International Symposium on Antennas and Propagation (ISAP), pp.541–542, 2021, doi: 10.23919/ISAP47053.2021.9391385.
- [10] B.K. Jung, N. Dreyer, J.M. Eckhard, and T. Kürner, "Simulation and automatic planning of 300 GHz backhaul links," 2019 44th International Conference on Infrared, Millimeter, and Terahertz Waves (IRMMW-THz), pp.1–3, 2019, doi: 10.1109/IRMMW-THz.2019.8873734.
- [11] B.K. Jung and T. Kürner, "Automatic planning algorithm of 300 GHz backhaul links using ring topology," 2021 15th European Conference on Antennas and Propagation (EuCAP), pp.1–5, 2021, doi: 10.23919/EuCAP51087.2021.9411010.
- [12] ThoR Deliverable, "D2.4 scenarios for demonstration and simulation," July 2019.
- [13] C. Bron and J. Kerbosch, "Algorithm 457: finding all cliques of an undirected graph," *Association for Computing Machinery*, pp.575–577, Sept. 1973.
- [14] D.M. Rose, J. Baumgarten, S. Hahn, and T. Kurner, "SiMoNe - Simulator for mobile networks: System-level simulations in the context of realistic scenarios," 2015 IEEE 81st Vehicular Technology Conference (VTC Spring), pp.1–7, 2015, doi: 10.1109/VTCSpring.2015.7146084.
- [15] B.K. Jung, C. Herold, J.M. Eckhardt, and T. Kürner, "Link-level and system-level simulation of 300 GHz wireless backhaul links," 2020 International Symposium on Antennas and Propagation (ISAP), pp.619–620, 2021, doi: 10.23919/ISAP47053.2021.9391508.
- [16] A. Fricke, S. Rey, B. Peng, T. Kürner, et al., "TG3d channel modelling document (CMD)," *IEEE 802.15 Document 15-14-0310-19-003d*, pp.1–61, 2016.
- [17] ITU-R P.676-12, "Attenuation by atmospheric gases and related effects," International Telecommunications Union, 2019.
- [18] ITU-R P.838-3, "Specific attenuation model for rain for use in prediction methods," International Telecommunications Union, 2005.
- [19] ITU-R P.840-8, "Attenuation due to clouds and fog," International Telecommunications Union, 2019.
- [20] T. Kürner, A. Hirata, B.K. Jung, E. Sasaki, P. Jurcik, and T. Kawanishi, "Towards propagation and channel models for the simulation and planning of 300 GHz backhaul/fronthaul links," 2020 XXXI-IIRD General Assembly and Scientific Symposium of the International Union of Radio Science, pp.1–4, 2020, doi: 10.23919/URSIGASS49373.2020.9232186.
- [21] ITU-R F.699-8, "Reference radiation patterns for fixed wireless system antennas for use in coordination studies and interference assessment in the frequency range from 100 MHz to about 86 GHz," International Telecommunications Union, 2018.
- [22] ITU-R F.1245-3, "Mathematical model of average and related radiation patterns for point-to-point fixed wireless system antennas for use in interference assessment in the frequency range from 1 GHz to about 86 GHz," 2019.
- [23] ThoR Deliverable, "D5.4 Planning rules of THz backhaul/fronthaul links," July 2021.
- [24] IEEE Standard association, "IEEE standard for high data rate wireless multi-media networks—Amendment 2: 100 Gb/s wireless switched point-to-point physical layer," *IEEE Std 802.15.3d-2017 (Amendment to IEEE Std 802.15.3-2016 as amended by IEEE Std 802.15.3e-2017)*, pp.1–55, 18 Oct. 2017, doi: 10.1109/IEEESTD.2017.8066476.



Bo Kum Jung received his B.E degree from Inha University, Incheon, Korea, in 2015, and the M.Sc. degree from the Technische Universität Braunschweig, Braunschweig, Germany, in 2019, and is a Ph.D. candidate at the Technische Universität Braunschweig.



Thomas Kürner received his Dipl.–Ing. degree in Electrical Engineering in 1990, and his Dr.–Ing. degree in 1993, both from University of Karlsruhe (Germany). Since 2003, he is a Full University Professor at the Technische Universität Braunschweig, working on simulation and modeling of mobile radio systems, including cellular networks, THz communications, and V2X communications. He was the chair of the IEEE 802.15.3d Task Group. Currently, he is chairing the IEEE 802.15 SC THz, is the EU coordinator of the EU-Japan Project ThoR and the spokesman of the DFG Research Unit Meteracom on Metrology for THz Communications.